



Title	Macropore Formation in Anodized p-Type Silicon and its Application to Field Emitter Arrays
Author(s)	Harada, Hiroshi; Shirahashi, Takuma; Nakamura, Mitsuhiro et al.
Citation	電気材料技術雑誌. 2001, 10(2), p. 79-82
Version Type	VoR
URL	https://hdl.handle.net/11094/81664
rights	
Note	

The University of Osaka Institutional Knowledge Archive : OUKA

<https://ir.library.osaka-u.ac.jp/>

The University of Osaka

Macropore Formation in Anodized p-Type Silicon and its Application to Field Emitter Arrays

Hiroshi Harada, Takuma Shirahashi, Mitsuhiro Nakamura, Takafumi Ohwada,
Akihiko Hosono¹, Soichiro Okuda¹ and Katsumi Yoshino²

Faculty of Science and Engineering, Shimane University
1060 Nishi-Kawatsu, Matsue, Shimane 690-8504 Japan

¹ Advanced Technology R&D Center, Mitsubishi Electric Corporation
8-1-1 Tsukaguchi-honmachi, Amagasaki, Hyogo 661-8661 Japan

² Faculty of Engineering, Osaka University
Yamada-oka, Suita, Osaka 565-0871 Japan

1. Introduction

Macropore formation in anodized p-type Si was first reported by Propst and Kohl¹⁾ in an absence of water and oxygen. They ascribed the formation mechanism of macropores to a preferential etching at a bottom of facet tips formed at an initial stage of anodization. Using a water contained electrolyte, several authors also observed macropores, however, top of those macropores was covered with a microporous Si layer²⁾ or pore volume was filled with microporous Si.³⁾

In this report it is described that macropores with an open pore and needles were observed in p-type Si anodized in a water contained electrolyte.⁴⁾ It is also shown that those macropores could be utilized to fabricate field emitter arrays (FEAs).

2. Experimental Procedure and Macropore Formation⁴⁾

The starting material was the p-type, (100), 17~23 $\Omega \cdot \text{cm}$, 20 cm Si wafer, whose back surface was mechanically ground to a thickness of 400 μm and then coated with successively deposited Ti/Ni/Au. Before the metal coating was performed, the wafers were divided into two groups termed A and B. Group A was exposed to the clean air ambient for 72 h at room temperature before the metal coating process, and group B was coated with the metal layer immediately after the grinding process. The only expected difference between groups A and B was in the formation process of the native oxide on the wafer. The thickness of the native oxide was measured by X-Ray Photoelectron Spectroscopy (XPS), and was determined to be 4.2 and 0.9 \AA for groups A and B, respectively. Before carrying out the anodic reaction, the wafer was cut into 33x33 mm^2 samples.

The anodic reaction was carried out at room temperature of 25 to 28°C, using the sample holder, in which the Au-plated Cu block was pressed to the back surface of the sample by a spring used for the electrical contact and the front surface of the sample was covered by a Teflon plug with a window through which the anodic reaction occurred. The electrolyte was 48 wt.% HF: de-ionized water (DI): isopropyl alcohol (IPA)=1:1:6 (vol.). In spite of the presence of the native oxide, the current flowed due to the tunnel effect. The current density of group A was slightly lower than that of group B at the same applied voltage. Figure 1 shows the current density vs. voltage characteristic of group A, in which the voltage was measured between the sample and the Pt counter electrode.

Anodization was carried out for 30 min, changing the current density from 0.5 to 63 mA/cm², and the anodized surface morphology was investigated by Scanning Electron Microscopy (SEM). SEM micrographs of both groups, A and B are shown in Fig.1. In the case of group A, the anodized surface was granular and its surface roughness was

less than $0.1\text{--}0.2 \mu\text{m}$ at current densities below 3 mA/cm^2 as seen in Fig.1(a). At current densities ranging between 10 to 40 mA/cm^2 , the anodized surface showed approximately rectangular parallelepiped macropores, which were orthogonal to the (100) surface as seen in Figs.1(c) and 1(C). A mixed structure of granular and macropore structures was observed at current densities ranging between 3 to 10 mA/cm^2 as seen in Fig.1(b). Above 40 mA/cm^2 , needle-like structures with diameters of $1.7 \mu\text{m}$ and heights of $12 \mu\text{m}$ were observed, as seen in Fig.1(d), followed by the mirror surface at 63 mA/cm^2 as seen in Fig.1(e). Dependences of the pitch and pore size of the macropore on the current density are shown in Fig.2. While the pitch was independent of the current density, the pore size increased with an increase of current density and approached that of the pitch above the current density of 40 mA/cm^2 . The formation of the needle-like structure above 40 mA/cm^2 is due to the disappearance of the walls of the macropores. The mirror surface at 63 mA/cm^2 may be attributed to the disappearance of both the walls and the beams at the corner of the macropores.

In the case of group B, a rugged surface was observed at current densities below 3 mA/cm^2 as seen in Figs.1(a') and 1(b'). Above current densities of 3 mA/cm^2 , the anodized surface was rough and both the macropore and needle-like structures were not observed as seen in Figs.1(c') and 1(d').

Though the detailed mechanism of the macropore formation is not clear at present, the preferential etching mechanism proposed by Propst and Kohl¹⁾ may be modified by changing the conditions of the back metallization.

3. Application to FEAs

We expected that the beams at corners of rectangular parallelepiped macropores might be modified to FEAs by a selective removal of pore walls. For the purpose, an anisotropic wet etching was carried out to macropores by using the etching solution of $1\text{mol KOH:IPA}=4.8:1$ (vol.) at 50°C . Etched surfaces observed by SEM are shown in Fig.3. Fig.3(a) and Fig.3(b) correspond to etching time of 10 and 15 min, respectively. As seen in Fig.3(a) and Fig.3(b), two types of projections, designated P1 and P2, were observed. The shapes of type P1 and P2 were the spear-like one and the ridge-like one, respectively. The ridges correspond to residual walls not fully removed. Coexistence of two types of P1 and P2 is presumed to be due to the variation of the thickness of the pore walls. With the increase of etching time, the ratio of type P1 to type P2 increased and the height of type P1 decreased. As seen in Fig.3(c), which was the plan view of Fig.3(b), most of the depressions in Fig.3(b) were the regular pyramid, whose base was parallel to (100). The average height of two types of projections measured from the base of the pyramid and the average pitch among projections in case of Fig.3(b) were $2.0 \mu\text{m}$ and $3.6 \mu\text{m}$, respectively. The magnified micrograph of the type P1 in Fig.3(b) is shown in Fig.3(d). It had a sharp tip, so we expected that an array of P1 and P2 projections might be utilized for an FEA.

Emission characteristics of the sample in the case of Fig.3(b) were measured in a vacuum chamber at a pressure of 1×10^{-8} Torr. The measurement system and a sample configuration are schematically shown in Fig.4. An anode was a glass coated with ITO (indium tin oxide) and phosphor of ZnO:Zn , whose size was $6\times 6 \text{ mm}^2$. The anode was separated approximately $90 \mu\text{m}$ apart from the sample by an insulating film (not depicted in Fig.4). The anode was positioned so that phosphor faced an area of the tip array in the sample, which was identical to an anodized area with a diameter of 8 mm. An emission current I was measured as a function of an applied voltage V between ITO and the sample. An emission started at a voltage of 800 V, which was the electric field of $9 \text{ V}/\mu\text{m}$ and the Fowler-Nordheim plot showed the linear characteristic as seen in Fig.5, which indicated that field emission from the sample could be

described by the Fowler-Nordheim theory. A cathode luminescence from the phosphor pattern at the applied electric field of $22 \text{ V}/\mu\text{m}$ is shown in Fig.6.

4. Conclusion

Using a water contained electrolyte, macropores and needles were observed in anodized p-type Si having a native oxide layer of 4.2 \AA between the back surface of Si and the back metal. Feasibility of an FEA made from the macropores was also confirmed.

Acknowledgements

The authors thank Mr.H.Yakushiji of Mitsubishi Electric Corp. for his help with the Si wafer preparation. The micrographs were taken using the SEM at the Cooperative Research Center of Shimane University.

- 1) E.K.Propst and P.K.Kohl: J.Electrochem.Soc.**141**(1994)1006.
- 2) R.B.Wehrspohn, J.-N.Chazalviel and F.Oznam: J.Electrochem.Soc.**145**(1998)2958.
- 3) V.Lehmann and S.R önnebeck: J.Electrochem.Soc.**146**(1999)2968.
- 4) H.Harada, T.Shirahashi, M.Nakamura, T.Ohwada, S.Sasaki, S. Okuda and A.Hosono: Jpn.J.Appl.Phys. **40**(2001)4862.

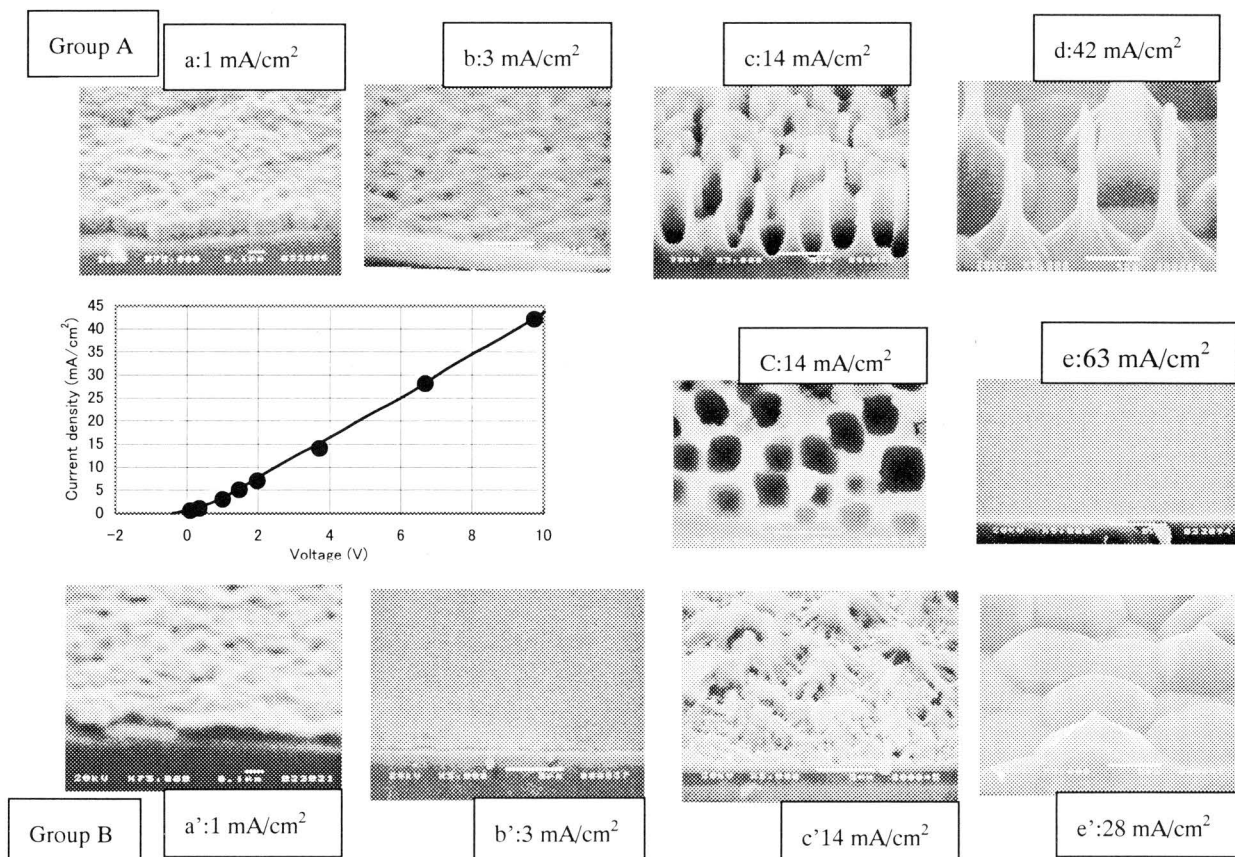


Fig.1 Current density vs voltage characteristics of group A and the anodized surface morphology observed by SEM. Top and middle micrographs are those of group A, and the bottom ones are of group B. For all micrographs, the tilt angle is 60 degree except that for the plan view of C. The white bar at the bottom of Figs. b-e, C and b'-d' is $5 \mu\text{m}$, and that in Figs. a and a' is $0.1 \mu\text{m}$.

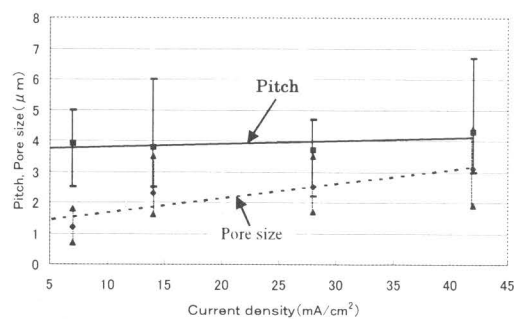


Fig.2 Pitch and pore size vs current density.

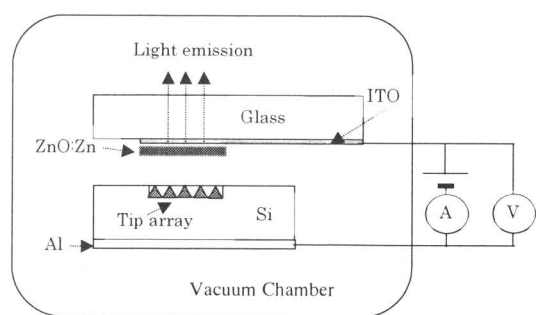


Fig.4 Schematic diagram of I-V measurement system.

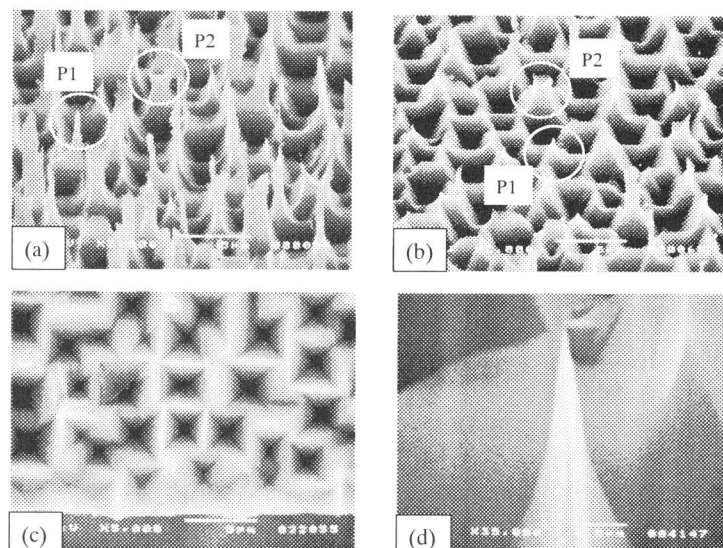


Fig.3 SEM micrographs of the etched surfaces of anodized macroporous Si; (a) etching time of 10 min, (b) etching time of 15 min, (c) plan view of (b) and (d) magnified micrograph of the type P1 projection in (b). P1 and P2 in (a) and (b) designate the type of projections. The tilt angle of (a), (b) and (d) was 60 degree.

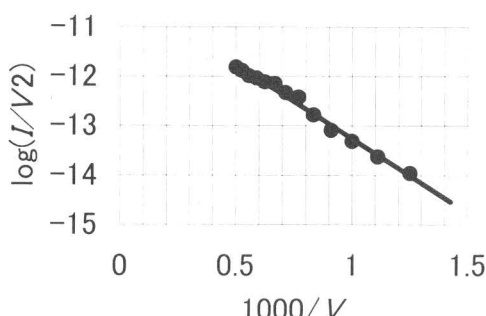


Fig.5 Fowler-Nordheim plot of the FEA made from macroporous Si.

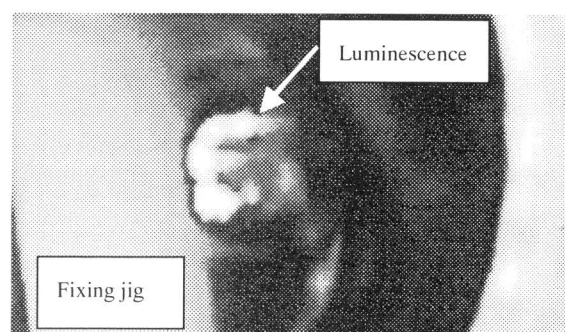


Fig.6 Cathode luminescence pattern from phosphor of ZnO:Zn, whose size was 6x6 mm².